Korean J. Chem. Eng., 32(12), 2456-2462 (2015)
DOI: 10.1007/s11814-015-0078-y

pISSN: 0256-1115
eISSN: 1975-7220

Preparation, structure and adsorption properties of synthesized multiwall carbon nanotubes for highly effective removal of maxilon blue dye

Ayad Fadhil Alkaim*,†, Zainab Sadik, Dunia Kamil Mahdi**, Saif Mohammed Alshrefi***, Abdulkareem Mohammed Al-Sammarraie****, Faisal Muhammad Alamgir*****, Preet Mohinder Singh*****, and Aseel Mushtaq Aljeboree***

*College of Science for Women-Chemistry Department, Babylon University, Hilla, Iraq
**College of Science-Physics Department, Baghdad University, Baghdad, Iraq
***College of Science for Women-Physics of Laser Department, Babylon University, Babylon, Iraq
****College of Science-Chemistry Department, Baghdad University, Baghdad, Iraq
*****School of Materials Science and Engineering, Georgia Institute of Technology, Altanta, GA 30332, USA
(*Received 21 December 2014 • accepted 13 April 2015*)

Abstract−Multiwall carbon nanotubes (MWCNTs) have been hydrothermally prepared using polyethylene glycol as the carbon source. Herein, new MWCNTs composites with high adsorption capacity were prepared and applied as efficient adsorbents for adsorption of maxilon blue dye (GRL) from aqueous solution. The morphologies of the MWCNTs were characterized by X-ray diffraction (XRD), Raman spectroscopy, scanning electron microscopy (SEM), transmission electron microscopy (TEM) and Fourier transform-infrared (FT-IR) spectroscopy. The adsorption property of maxilon blue (GRL) from aqueous solution onto MWCNTs was studied as a function of mass dosage, pH of solution, initial dye concentration and temperature. The adsorption of GRL depends on the initial pH of the solution with maximum uptake occurring at about pH 10. The maximum adsorption capacity of prepared MWCNTs was 260.7 mg/g. Langmuir, Freundlich and Temkin isotherms were applied to fit the experimental data. The Freundlich equilibrium isotherm fitted well the experimental data indicating the homogeneity of the adsorbent surface sites. Thermodynamics parameters were studied the changes in free energy (ΔG^0), enthalpy (ΔH^0) and entropy (ΔS^0) during adsorption. It is noticeable that the adsorption of GRL dye onto MWCNTs was a spontaneous and endothermic process and indicates that the adsorption is favored at high temperature.

Keywords: Multiwall Carbon Nanotube, Hydrothermal, Adsorption, Maxilon Blue Dye

INTRODUCTION

Many important industries, such as textile, feedstuffs, paper, leather, cosmetics, among others, use dyes for coloring their final products [1], and consequently produce large amounts of dye-containing effluents. The presence of dye containing waters can adversely affect the aquatic environment by impeding light penetration, precluding photosynthesis of aquatic flora [2]. Moreover, most of the dyes can cause dermatitis, allergy, and skin irritation and can also provoke cell mutation. Synthetic dyes belong to a class of organic compound with a complex aromatic molecular structure that can provide bright and firm color to industrialized products. However, the complex aromatic molecular structures of dyes make them more stable and difficult to biodegrade [3]. Therefore, water pollution becomes one of the most serious environmental problems, so the treatment and disposal of wastewater has aroused widespread concern. Adsorption technology is thought as one of the most effective methods to remove pollutants from aqueous solutions, because it is simple, convenient, and low cost with high sorption efficiency and wide adaptability [4,5].

Different adsorbents have been used for the removal of dyes from aqueous solutions [6-8]. Carbon nanotubes (CNTs), as an important category of nanomaterials, have received increasing attention in recent years [9]. CNTs were widely used in all kinds of products due to their extraordinary electrical, chemical, and physical properties [10]. Therefore, carbon nanotubes (CNTs) happen to be among the adsorbents that have been employed for the successful removal of dyes from aqueous effluents [11-15].

Carbon nanotubes are divided into two general types: single-wall carbon nanotubes (SWCNTs) and multi-wall carbon nanotubes (MWCNTs). CNTs are attractive alternative adsorbents for the removal of dye contaminants from aqueous effluents because they possess large specific surface area, small size as well as hollow, layered structures, and remarkable electrical conductivities giving rise to adsorbents with much higher sorption capacity when compared with ordinary adsorbents [16-19].

In this study, synthesized multiwall carbon nanotubes were used to study the removal/adsorption of maxilon blue dye from an aqueous solution. The effects of various operating parameters, such as mass of the multiwall carbon nanotubes, solution pH, temperature, and dye concentration, were studied and optimized. Thermodynamic calculations of the adsorption process are required to understand the mechanism of adsorption, spontaneity, and heat of adsorption using different thermodynamic parameters, also adsorp-

†To whom correspondence should be addressed.
E-mail: alkaim@iftc.uni-hannover.de

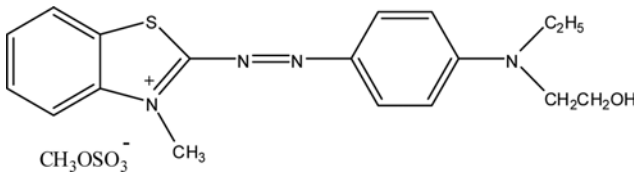

Fig. 1. Chemical structure of maxilon blue (GRL).

tion isotherms were also evaluated and reported.

EXPERIMENTAL

1. Materials

Ethanol (Sigma-Aldrich), polyethylene glycol (PEG) 40% (w/w) in H_2O, average M.wt. 8,000 (Sigma-Aldrich), sodium hydroxide ACS reagent, ≥97.0%, Palladium(II) chloride 99.999% (Aldrich), Maxilon blue GRL [λmax=599 nm] was obtained from Al-Hilla/ Textile Company (Babylon, Iraq). The chemical structure of maxilon blue GRL is shown in Fig. 1, all of materials have been used without further purifications. All aqueous solutions have been prepared with deionized water from a SARTORIUS ARIUM 611 apparatus.

2. Synthesis of MWCNTs

Typically, 1 g of $PdCl_2$, 2.4 g NaOH and 6 g PEG were dissolved in (100 ml) of alcoholic aqueous solution 90%, then sonicated for 10 min. The resulting solution was transferred into a 250 mL Teflon cup [20]. Afterwards, the Teflon cup was sealed in an autoclave and placed into an electric furnace held at 190 °C for 24 h. Finally, the autoclave was naturally cooled in air. The resulting carbon nanotubes were separated by centrifugation, and washing by ethanol, then distilled water for several times, and then dried overnight in an oven at 60 °C.

3. Characterization Techniques

XRD measurements were made with a Siemens Diffractometer Model D-5000, using CuKα radiation and operated at 40 kV and 20 mA with a $\theta/2\theta$ mode, Raman spectrum (Thermo Nicolet), Scanning electron microscopy (SEM) was on a field emission scanning microscope model Zeiss ULTRA 60 FE-SEM working under low accelerating voltage, 2-5 kV, and transmission electron microscopy (JEOL 100CX II (TEM) 100 kV) were used to determine the structural characteristics of the nanocomposites on the nanometer domain.

4. Batch Equilibrium Studies

4-1. The Effect of the Adsorbent Dose and the Optimal Concentration

The effect of MWCNTs dosage on the dye adsorption was investigated by adding various dosages of MWCNTs (25-300 mg/L) to initial dye concentrations (50 mg/L) at the contact time of 120 min and pH=6. Also, to determine the effect of the initial dye concentration on the adsorption process, various dye concentrations (5, 10, 15, 25, 40, 50, 60, 75 and 100 mg/L), constant pH 6, contact time of 120 min, and dose of the adsorbent (100 mg/L).

4-2. The Effect of pH

At first, the solution pH range (2-10) was set and the experiments were performed on the dye concentration of 50 mg/L, a fixed adsorbent dose (100 mg/L), and contact times (120 min). Then, samples were obtained from the solutions and the efficiency was evaluated.

4-3. The Effect of Temperature

To assess the effect of the temperature on the equilibrium adsorption capacity of GRL, the adsorption studies were carried out at different temperatures (10, 20, 30 and 50 °C), dye concentration (50 mg/L), pH=6, contact time of 120 min, and 100 mg/L of the adsorbent. Afterwards, samples were obtained from the solutions and the efficiency was measured.

At the end of the equilibrium period, the suspensions were separated for later analysis of the dye concentration. The liquid dye solution was separated from the MWCNT solid phase by centrifuge in 3,500 rpm and 10 min. The amount of GRL adsorption at equilibrium q_e (mg/g) was calculated from the following equation:

$$q_e = \frac{V(C_0 - C_e)}{W} \quad (1)$$

The removal percentage of each GRL dye was calculated as follows:

$$\text{Removal } \% = \frac{(C_0 - C_e)}{C_0} \times 100 \quad (2)$$

where C_0 and C_e (mg/L) are the liquid phase concentrations of dye at initial and equilibrium, respectively, V (L) the volume of the solution and W (g) is the mass of adsorbent used. The concentration of GRL after and before adsorption was determined using a spectrophotometer at λ_{max}=599 nm.

RESULTS AND DISCUSSION

1. Characterization

XRD analysis usually involves the identification of phases in a given sample. XRD patterns of the as synthesis MWCNTs sample are shown in Fig. 2. The pattern indicates the existence of the graphite peak at 26.5 as assigned earlier [21]. As shown, the strongest diffraction peak at 26.5°, peaks with medium intensity at 44.6°,

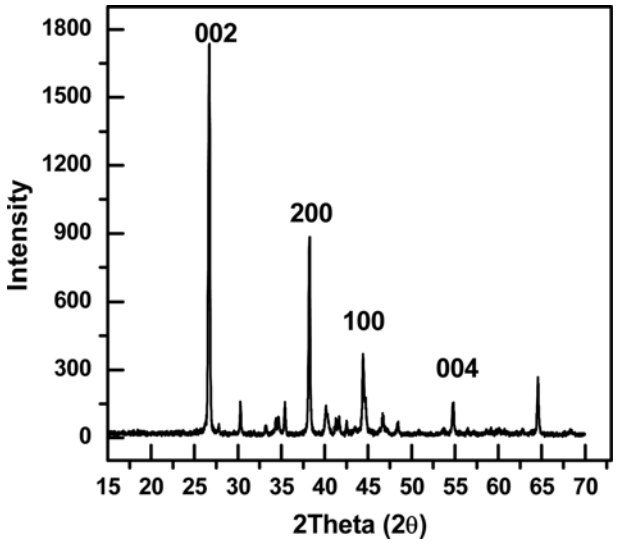

Fig. 2. XRD pattern of synthesized MWCNTs.

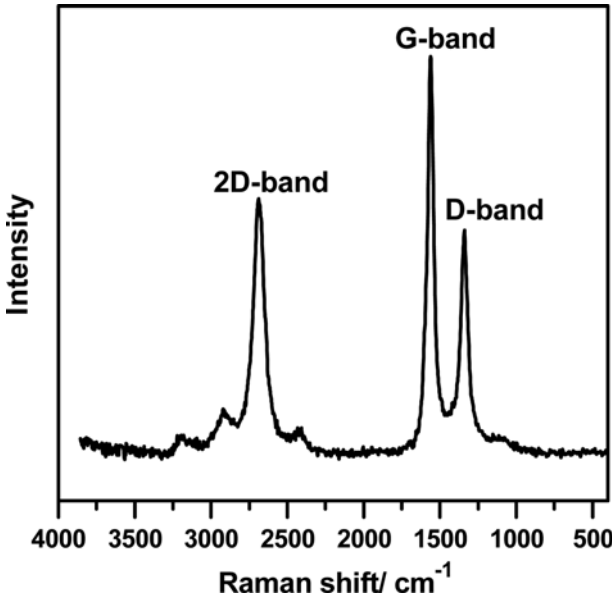

Fig. 3. Raman spectrum of synthesized MWCNTs.

and weak peaks at 54.2° can be well indexed as the (002), (100), and (004) reflections of graphite, respectively [22,23]. Similar findings have been reported by other researchers [24-26]. There is strong peak at 36.6 which could be an indicator for the presence of Pd catalyst component in the as grown MWCNTs sample.

Raman spectroscopy is an important technique to investigate the crystal structure of CNTs. The characteristic peaks of MWCNTs were observed at 1,347.11 cm^{-1} (D band), 1,559 cm^{-1} (G band) and 2,705 cm^{-1} (2D band) as presented in Fig. 3. The D band is attributed to the disorder induced A_1g Raman mode [27] and the G band corresponds to the Raman-active E_2g vibration of neighboring sp^2 carbon atoms [28]; its intensity represents the degree of graphitization in the material. The intensity ratio of the D band to the G band (ID/IG) is used as a measure of structural quality of graphite-like materials, whereas the 2D band is the overtone of the D band but independent of crystalline defects [29].

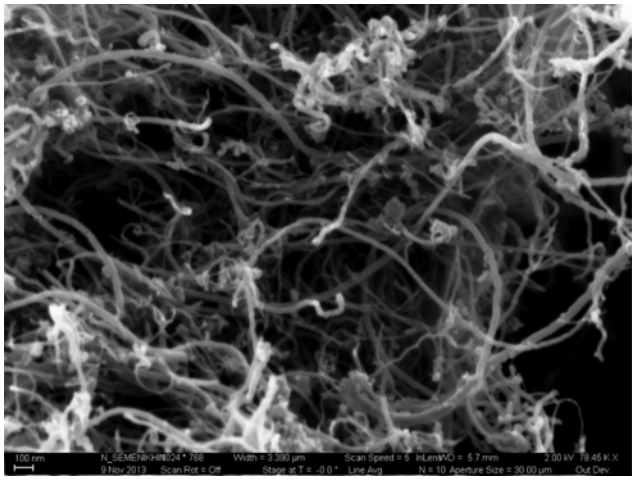

Fig. 4. SEM images of synthesized MWCNTs.

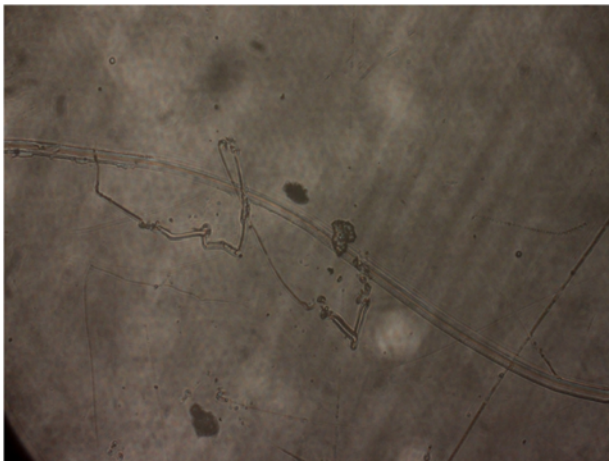

Fig. 5. TEM images of synthesized MWCNTs.

Scanning electron microscopy (SEM) imaging was also used to characterize the surface morphology of multiwalled carbon nanotubes. Fig. 4 displays the SEM images of raw MWCNTs. It is evident from the Fig. 4 that the MWCNTs are cylindrical, curved and tangled together [30].

Fig. 5 shows the transmission electron microscope image (TEM) of the synthesized MWCNTs. The MWCNTs were long and entangled around each other with an average diameter between 20 and 50 nm and an average length between 2 and 5 μm. The TEM analysis verified the hollow structure of MWCNTs used and showed that the inner diameter was between 6 and 10 nm with clear surface.

2. Batch Equilibrium Studies

2-1. Effect of Adsorbent Dosage

The effect of MWCNT dosage is depicted in Fig. 6. Evidently, percentage removal increased with the increase of the sorbent mass and the uptake capacity of GRL dye decreased from 260.22 mg/g (13.01% removal) to 96.65 mg/g (57.99% removal) with increas-

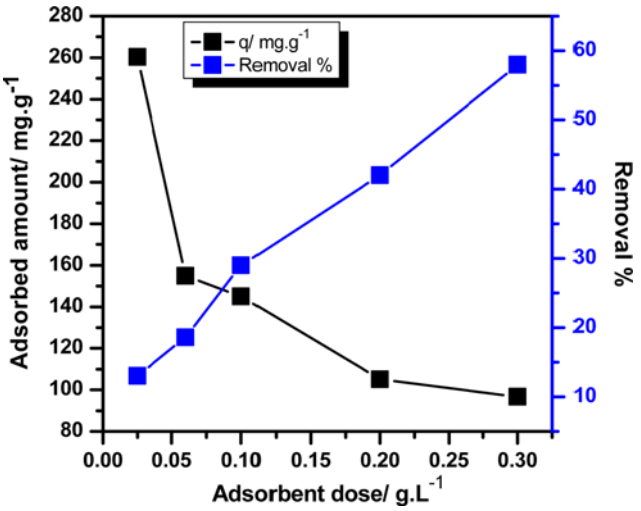

Fig. 6. The effect of MWCNTs/dose on the removal of GRL dye (experimental conditions: 120 min, 303 K, pH 6, and GRL concentration 50 mg L^{-1}).

ing MWCNT concentration from 25 to 300 mg/L (Fig. 6). The increase in the percentage of maxilon blue dye removed from the aqueous solution is primarily due to the greater number of active sites available for adsorption as a result of the increased amount of MWCNTs present [31].

2-2. Effect of pH

The pH of the dye solution affects not only the surface charge of the MWCNTs surface adsorbent, the degree of ionization of the materials and the dissociation of functional groups on the active sites of the adsorbents surface, but also the structure of the dye molecule [32]. The pH effect (2.0-10.0) on the adsorption of GRL on MWCNTs was evaluated using MWCNTs dosage 100 mg L^{-1}, initial dye concentration of 50 mg L^{-1}, temperature 303 K, and contact time of 2 h.

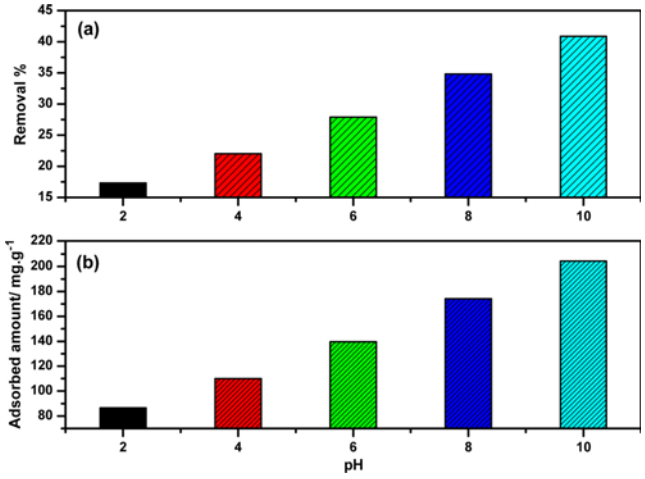

Fig. 7. The effect of solution pH on the removal of perecentage and adsorption capacity (Fig. 7(a), and Fig. 7(b) respectivelly) for adsorption of GRL by MWCNTs (experimental conditions: 120 min, 303 K, 0.1 g·L^{-1} MWCNTs, and GRL concentration 50 mg L^{-1}).

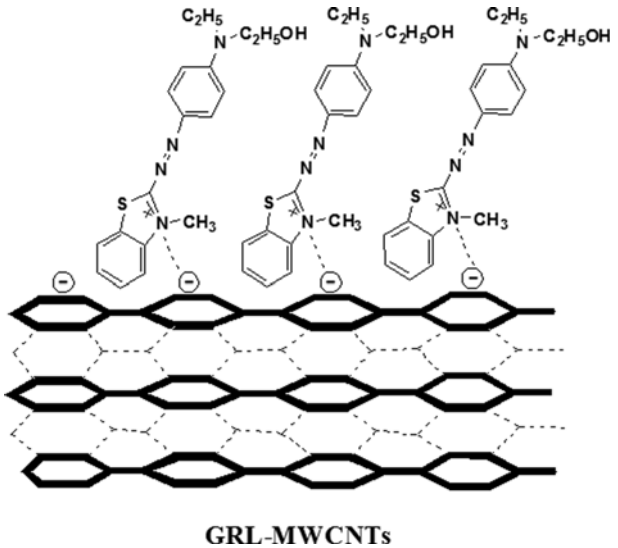

Scheme 1. GRL dye adsorption on MWCNTs with at pH higher than 6.

As shown in Fig. 7, dye removal efficiency increased when the pH increased from 2 to 10, indicating that pH significantly affected GRL removal percentage, particularly under basic conditions.

For a chosen dye concentration, 50 mg L^{-1} removal of GRL decreased from 15 to 46% when the pH increased from 2 to 10. The dissolved GRL dye is positively charged in water solution, and then the removal of this dye takes place when the adsorbents present a negative surface charge. Basic condition increases the electrostatic attraction between cationic dye and partially negative charged MWCNTs surface; therefore, the increase of the pH value (basic condition) the number of negatively charged sites increases and the number of positively charged sites decreases [33], While lower adsorption of GRL by surfaces adsorbents at low pH values may be explained by the competition of excess H^+ ions with the dye cation for active adsorption sites [31]. The adsorption mechanism of the GRL on MWCNTs can be illustrated in Scheme 1.

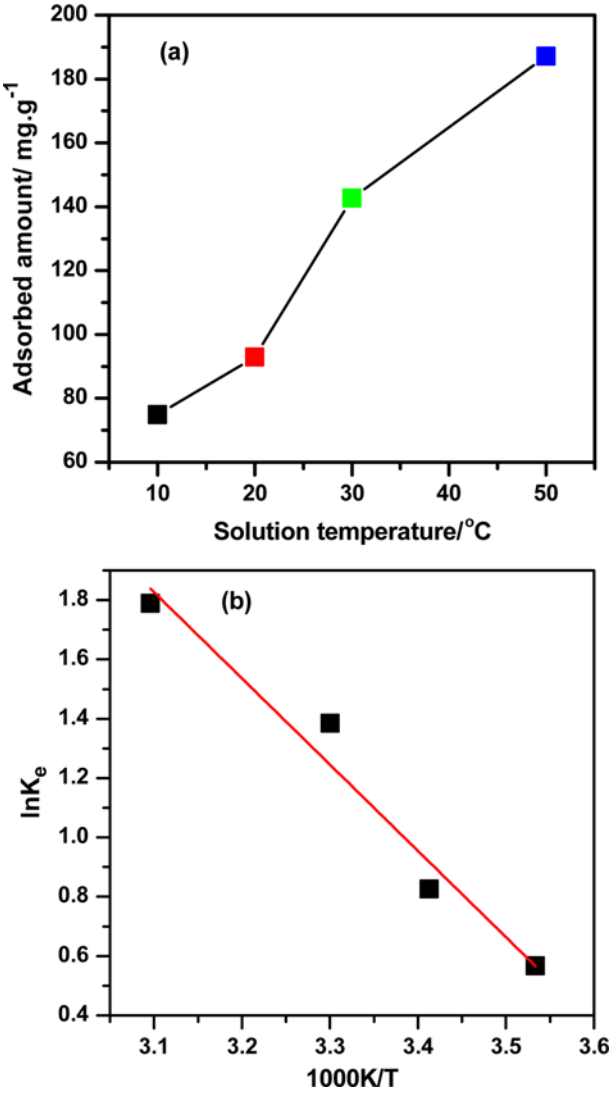

Fig. 8. (a) Effect of temperature on adsorption of the GRL onto MWCNTs (experimental conditions: 120 min, pH 6, 0.1 g·L^{-1} MWCNTs, and GRL concentration 50 mg L^{-1}), (b) van't Hoff plot for the adsorption of the GRL onto MWCNTs.

2-3. Effect of Temperature

The temperature of the solution was considered to be a critical factor affecting the adsorption process. If the removal efficiency of a certain pollutant from an aqueous solution is temperature dependent, which occurs in most cases, then it might affect the suitability of the adsorbent.

Various dye effluents are produced at relatively high temperatures [34]. Therefore, to determine the effect of temperature, adsorption experiments were carried out at 10, 20, 30 and 50 °C, respectively. As shown in Fig. 8(a), the adsorption capacity increases with the increase in temperature. The maximum adsorption capacity increases from 72.4 to 189.6 mg g^{-1} with the increase in temperature from 10 to 50 °C, which illustrates that the adsorption process of GRL onto MWCNTs is endothermic.

The increase in adsorption capacity of MWCNTs at higher temperature may be attributed to the enhanced mobility and penetration of dye molecules within the sorbent porous structure overcoming the activation energy barrier and enhancing the rate of intraparticle diffusion [35,36].

2-4. Thermodynamic Results

The thermodynamic parameters provide in-depth information about the energetic changes associated with adsorption process. To study the thermodynamics of adsorption of GRL dye on MWCNTs, the adsorption was evaluated by the equilibrium constant (K_e), enthalpy (ΔH^o), entropy (ΔS^o) and Gibbs free energy (ΔG^o) using following equations [37]:

$$K_e = \frac{q_e}{C_e} \tag{3}$$

$$\Delta G^o = -RT\ln K_e \tag{4}$$

$$\ln K_e = \frac{\Delta S^o}{R} + \frac{\Delta H^o}{RT} \tag{5}$$

where K_e is the equilibrium constant, T is the temperature, and R is the gas constant, respectively. ΔH^o and ΔS^o are calculated from the slope and intercept of van't Hoff plots of ln K_e vs T^{-1} (Fig. 8(b)).

The calculated thermodynamic parameters are tabulated in Table 1, the negative Gibbs free energy change (ΔG^o) and the positive value of (ΔH^o), indicating that the adsorption process is spontaneous and endothermic, respectively. Further, the positive value of entropy change (ΔS^o) reflects the random nature of process at the solid/solution interface and the affinity of MWCNTs for GRL adsorption [34,38]. The randomness at the solid-solution interface may be due to the more translational entropy gained by the displaced water molecules as compared to that lost by the dye molecules during the adsorption process [39].

Table 1. Thermodynamic parameters for the adsorption of GRL on the surface of synthesized MWCNTs

T/K	K_e/L·g^{-1}	ΔG/ kJ·mol^{-1}	ΔH/kJ·mol^{-1}	ΔS/J·K^{-1}·mol^{-1}
283	1.76±0.01	−1.33±0.09	24.17±0.41	90.0 4±1.63
293	2.28±0.06	−2.01±0.17		
303	3.99±0.09	−3.48±0.23		
323	5.98±0.12	−4.80±0.31		

3. Adsorption Isotherms

Adsorption isotherm is helpful in describing the interaction of adsorbates with adsorbents, and the equilibrium distribution of adsorbate molecules between the liquid and solid phases. It is therefore critical for the optimal utilization of adsorbents. In this study, three isotherm models, Langmuir, Freundlich and Temkin equations, were applied to simulate the isotherm data. The Langmuir isotherm model [40] is based on the assumption of a homogeneous adsorbent surface with identical adsorption sites:

$$q_e = \frac{q_m K_L C_e}{1 + K_L C_e} \tag{6}$$

where C_e (mg L^{-1}) is the equilibrium concentration of GRL, q_m (mg g^{-1}) is the maximum adsorption capacity and K_L (L mg^{-1}) is a constant related to the free energy of adsorption. The Freundlich model [41] is an empirical equation assuming heterogeneous adsorbent surface given by Eq. (7):

$$q_e = K_F C_e^{1/n} \tag{7}$$

where K_F and n are Freundlich parameters related to the adsorption capacity and adsorption intensity, respectively. The Temkin isotherm equation [42] shows the effects of indirect interactions between adsorbate molecules based on the assumption that the heat of adsorption of all molecules in the layer would decrease linearly with surface coverage. It has predictive power over a wide range of concentrations and is commonly expressed as:

$$q_e = B\ln(AC_e) \tag{8}$$

where B=RT/b and b (J mol^{-1}) is the Temkin constant related to the heat of adsorption; A (L g^{-1}) is the Temkin isotherm constant, R (8.314 J mol^{-1} K^{-1}) is the universal gas constant where T (K) is the absolute temperature. The nonlinear fitting of the three iso-

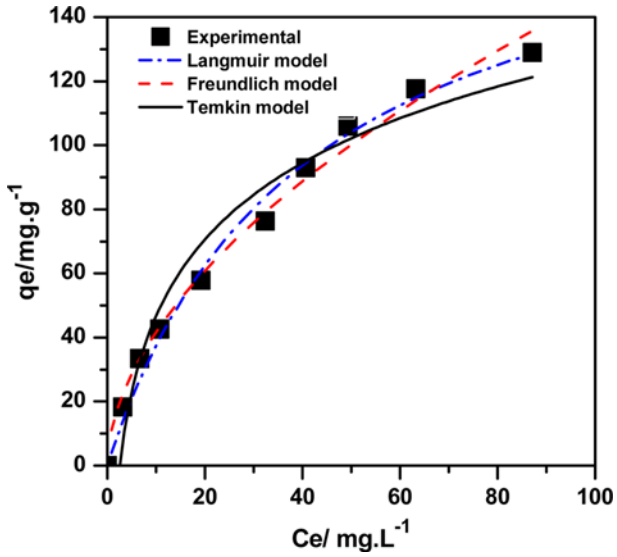

Fig. 9. Different adsorption isotherm models (Langmuir, Freundlich and Temkin) fit for adsorption of GRL dye on MWCNTs (experimental conditions: 120 min, 303 K, pH 6, 293 K, and 0.1 g·L^{-1} MWCNTs).

Table 2. Langmuir, Freundlich and Temkin model isotherms parameters for GRL adsorbed on the surface of synthesized MWCNTs

Isotherm models	Parameters	Value	SD
Langmuir	q_m (mg·g^{-1})	187.69	13.09
	K_L (L·mg^{-1})	0.024	0.0038
	R^2	0.98568	
Freundlich	K_F	11.84	1.331
	1/n	0.54	0.028
	R^2	0.98741	
Temkin	B/J·mole^{-1}	0.388	0.072
	K_T	34.45	2.6437
	R^2	0.9641	

therm models for the adsorption of GRL onto MWCNTs at 20 °C in fitting with Eqs. (6), (7) and (8) is depicted in Fig. 9.

The isotherm parameters were determined from the slopes and intercepts; standard deviation (SD) together with the correlation coefficients (R^2) are listed in Table 2. Results obtained with the nonlinear fitting show that the adsorption data could be best fitted to the Freundlich and Langmuir isotherm model. This implies that the adsorption of GRL onto MWCNTs from aqueous solutions proceeds by a monolayer formation.

CONCLUSION

A low-temperature hydrothermal route has been successfully developed to synthesize MWCNTs at 190 °C with catalyst Pd by using PEG as the carbon source. The diameters of the as-prepared MWCNTs are smaller than those prepared by high-temperature hydrothermal method. The effect of varying parameters that affect the removal/adsorption process such as mass dosage of MWCNTs, pH of solution, temperature, and initial GRL concentration were investigated. The amount of GRL dye adsorbed per unit MWCNTs mass increased with increases in pH of solution, initial dye concentration, and temperature. Equilibrium isotherm data were fitted using Langmuir, Freundlich, and Temkin models. Among these models, Freundlich and Langmuir models are in good agreement with the experimental data with high R^2. The adsorption of GRL dependence on temperature was investigated and the thermodynamic parameters ΔG^0, ΔH^0 and ΔS^0 were calculated. The negative ΔG^0 value indicated that the adsorption was feasible and spontaneous. The positive ΔH^0 and ΔS^0 values depicted endothermic nature of the adsorption and the affinity of MWCNTs for GRL adsorption, respectively. The mechanism of adsorption includes mainly electrostatic interactions (physical interactions) between GRL and MWCNTs. So the adsorption is a physisorption process. This study concluded that MWCNTs are an appropriate adsorbent for removing maxilon blue dye from wastewater.

ACKNOWLEDGEMENTS

This project was financial support by Babylon University, College for Women science-chemistry department, Hilla /Iraq.

REFERENCES

1. B. Royer, N. F. Cardoso, E. C. Lima, T. R. Macedo and C. Airoldi, *J. Hazard. Mater.*, **181**, 366 (2010).
2. N. F. Cardoso, E. C. Lima, B. Royer, M. V. Bach, G. L. Dotto, L. A. Pinto and T. Calvete, *J. Hazard. Mater.*, **241-242**, 146 (2012).
3. L. T. Prola, E. Acayanka, E. C. Lima, C. S. Umpierres, J. P. Vaghetti, W. O. Santos, S. Laminsi and P. T. Djifon, *Ind. Crop. Prod.*, **46**, 328 (2013).
4. Y. Wang and W. Chu, *Ind. Eng. Chem. Res.*, **50**, 8734 (2011).
5. J. Hu, D. Shao, C. Chen, G. Sheng, X. Ren and X. Wang, *J. Hazard. Mater.*, **185**, 463 (2011).
6. A. M. Aljebori and A. N. Alshirifi, *Asian J. Chem.*, **24**, 5813 (2012).
7. M. Shirzad-Siboni, A. Khataee, F. Vafaei and S. Joo, *Korean J. Chem. Eng.*, **31**, 1451 (2014).
8. R. Lafi, A. ben Fradj, A. Hafiane and B. H. Hameed, *Korean J. Chem. Eng.*, **31**, 2198 (2014).
9. G. S. Simate, S. E. Iyuke, S. Ndlovu, M. Heydenrych and L. F. Walubita, *Environ. Int.*, **39**, 38 (2012).
10. W. Sun, B. Jiang, F. Wang and N. Xu, *Chem. Eng. J.*, **264**, 645 (2015).
11. S. Chatterjee, T. Chatterjee, S. Lim and S. H. Woo, *Bioresour. Technol.*, **102**, 4402 (2011).
12. L. T. Prola, F. M. Machado, C. P. Bergmann, F. E. de Souza, C. R. Gally, E. C. Lima, M. A. Adebayo, S. L. P. Dias and T. Calvete, *J. Environ. Manage.*, **130**, 166 (2013).
13. M. A. Baghapour, S. Pourfadakari and A. H. Mahvi, *J. Ind. Eng. Chem.*, **20**, 2921 (2014).
14. M. A. Salam, R. M. El-Shishtawy and A. Y. Obaid, *J. Ind. Eng. Chem.*, **20**, 3559 (2014).
15. M. Shirmardi, A. H. Mahvi, B. Hashemzadeh, A. Naeimabadi, G. Hassani and M. V. Niri, *Korean J. Chem. Eng.*, **8**, 1603 (2013).
16. F. M. Machado, C. P. Bergmann, T. M. Fernandes, E. C. Lima, B. Royer, T. Calvete and S. B. Fagan, *J. Hazard. Mater.*, **192**, 1122 (2011).
17. J. Gong, J. Feng, J. Liu, Z. Jiang, X. Chen, E. Mijowska, X. Wen and T. Tang, *Chem. Eng. J.*, **248**, 27 (2014).
18. J. Cheng, P. R. Chang, P. Zheng and X. Ma, *Ind. Eng. Chem. Res.*, **53**, 1415 (2014).
19. F. M. Machado, C. P. Bergmann, T. H. Fernandes, E. C. Lima, B. Royer, T. Calvete and S. B. Fagan, *J. Hazard. Mater.*, **192**, 1122 (2011).
20. W. Wang, J. Y. Huang, D. Z. Wang and Z. F. Ren, *Carbon*, **43**, 1328 (2005).
21. M. Morsy, M. Helal, M. El-Okr and M. Ibrahim, *Spectrochim. Acta A*, **132**, 594 (2014).
22. S. Akbayrak and S. Ozkar, *Appl. Mater. Interfaces*, **4**, 6302 (2012).
23. Z. Sun, X. Zhang, Na, Z. Liu, B. Han and G. An, *J. Phys. Chem. B*, **110**, 13410 (2006).
24. C. Chen, J. Hu, D. Shao, J. Li and X. Wang, *J. Hazard. Mater.*, **164**, 923 (2009).
25. V. K. Gupta, S. Agarwal and T. A. Saleh, *J. Hazard. Mater.*, **185**, 17 (2011).
26. W. Oh, F. Zhang and M. Chen, *J. Ind. Eng. Chem.*, **16**, 321 (2010).
27. S. Osswald, E. Flahaut, H. Ye and Y. Gogotsi, *Chem. Phys. Lett.*, **402**, 422 (2005).
28. P. C. Eklund, J. M. Holden and R. A. Jishi, *Carbon*, **33**, 959 (1995).

29. R. Saito, A. Gruneis, G. G. Samsonidze, V. W. Brar, G. Dresselhaus, M. S. Dresselhaus, A. Jorio, L. G. Cancado, C. Fantini, M. A. Pimenta and A. G. Souza Filho, *New J. Phys.*, **5**, 157 (2003).
30. M. A. Salam, M. I. Makki and M. A. Abdelaal, *J. Alloy. Compd.*, **509**, 2582 (2011).
31. A. M. Aljeboree, A. F. Alkaim and A. H. Al-Dujaili, *Desalin. Water Treat.*, **53**, 3656 (2015).
32. Y. Lin and J. Leu, *Bio. Chem. Eng. J.*, **39**, 457 (2008).
33. Y. Li, Q. Du, T. Liu, X. Peng, J. Wang, J. Sun, Y. Wang, S. Wu, Z. Wang, Y. Xia and L. Xia, *Chem. Eng. Res. Des.*, **91**, 361 (2013).
34. M. Peydayesh and A. Rahbar-Kelishami, *J. Ind. Eng. Chem.*, **21**, 1014 (2015).
35. Z. Aksu and E. Kabasakal, *Sep. Purif. Technol.*, **35**, 223 (2004).
36. M. Kara, H. Yuzer, E. Sabah, M. S. Celik, *Water Res.*, **37**, 224 (2003).
37. L. Ai, M. Li, L. Li, *J. Chem. Eng. Data*, **56**, 3475 (2011).
38. V. Rocher, J. Siaugue, V. Cabuil and A. Bee, *Water Res.*, **42**, 1290 (2008).
39. S. M. Musyoka, H. Mittal, S. B. Mishra and J. C. Ngila, *Int. J. Biol. Macromol.*, **65**, 389 (2014).
40. I. Langmuir, *J. Am. Chem. Soc.*, **40**, 1361 (1918).
41. V. O. Njoku, K. Y. Foo, M. Asif and B. H. Hameed, *Chem. Eng. J.*, **250**, 198 (2014).
42. M. J. Temkin and V. Pyzhev, *Acta Physiochem. USSR*, **12**, 217 (1940).